ACTA IMEKO
ISSN: 2221-870X
September 2024, Volume 13, Number 3, 1 - 9

Artificial aging of monoazo and isoindoline yellow pigments

Agnese De Carlo[1,2,3,4], Valerio Graziani[3,4], Antonella Privitera[1], Armida Sodo[1], Paolo Branchini[3,4], Patrizio Antici[2], Luca Tortora[1,3,4]

[1] *Department of Science, Roma Tre University, via della Vasca Navale 84 00146 Rome, Italy*
[2] *INRS-EMT, 1650 Blvd. Lionel-Boulet, Varennes, QC, J3X 1P7, Canada*
[3] *National Institute for Nuclear Physics INFN — Roma Tre Division, via della Vasca Navale 84 00146 Rome, Italy*
[4] *Surface Analysis Laboratory Roma Tre LASR3, via della Vasca Navale 84 00146 Rome, Italy*

ABSTRACT
UV- and humidity-related aging effects on two yellow synthetic organic pigments, known for their good lightfastness, were investigated: Pigment Yellow 1 (PY 1, Monoazo) and Pigment Yellow 139 (PY 139, Isoindoline). The work considers the reactivity of these pigments, as individual pigments, in combination with linseed oil, and in presence of highly reactive inorganic white pigments: basic lead carbonate, titanium dioxide, and zinc oxide. Accelerated aging was induced via UV irradiation and high humidity rate in a custom-built chamber using both simple and bilayer paint mock-ups to simulate the technique of overlaying films in paintings. After aging, physicochemical variations were analysed using colorimetry, Fourier-transform infrared spectroscopy, Raman spectroscopy, and photoluminescence spectroscopy. The results show that the accelerated aging induces a greater colour change in monoazo yellow pigment than in isoindoline one when in powder form. Conversely, when oil is present in the samples as binder, the colour variations are similar for both samples suggesting that the large part of the chemical/physical changes occur in the organic binder. For the bilayer systems, photoluminescence spectroscopy suggests that the substrates can induce a larger drying activity on the binder and could follow the contribution of fluorescence in the variation of the perceived colour.

Section: RESEARCH PAPER

Keywords: artificial aging; synthetic organic pigments; monoazo; isoindoline; inorganic whites; linseed oil; lightfastness; bilayer mock-ups; measurement

Citation: A. De Carlo, V. Graziani, A. Privitera, A. Sodo, P. Branchini, P. Antici, L, Tortora , Artificial aging of monoazo and isoindoline yellow pigments, Acta IMEKO, vol. 13 (2024) no. 3, pp. 1-9. DOI: 10.21014/actaimeko.v13i3.1791

Section Editor: Fabio Leccese, Università Degli Studi Roma Tre, Rome, Italy

Received February 22, 2024; **In final form** May 13, 2024; **Published** September 2024

Funding: This work was supported by "GRAL - Green and Long-lasting stone conservation products" project (n. F85F21001710009) in the call "Progetto Gruppi di Ricerca 2020" by Regione Lazio.

Corresponding author: Agnese De Carlo, e-mail: agnese.decarlo@uniroma3.it

1. INTRODUCTION

An artist tries to communicate through a work of art with the use of colours. However, our eyes can barely see the original intent of the artist. Color changes, like fading, darkening, and blanching [1], [2] can occur as a consequence of physical and chemical photodegradation processes [3], due to exposure to light and environmental factors. Understanding the processes occurring in materials used by artists and their aging mechanisms is fundamental for preserving artworks [4], [5]. For this reason, many studies focused on pigment aging and light stability, known as lightfastness [6]-[8].

Two yellow pigments from different classes of synthetic organic compounds - monoazo and isoindoline – were chosen for this study and were analysed pre- and post-aging. The American Society of Testing and Materials, ASTM International, lists these two pigments among those with high stability and good lightfastness when combined with oil [9]-[11].

Nonetheless, a comprehensive understanding of the lightfastness in the case of powder pigments or paints interacting with inorganic white pigments as substrates is still lacking. Indeed, the inorganic compounds can be reactive with the binder [12], leading to colour changes [4] or to the formation of metal soaps in the paint layers [13].

Monoazo pigments represent one of the earliest examples of synthetic organic yellow pigments, whereas isoindoline pigments are categorized among the most recent ones. Monoazo pigments find widespread utilization across diverse applications, such as paints and textile printings, owing to their commendable lightfastness and resistance [14]. On the other hand, the isoindoline pigments find applications in plastics, paints, printing

inks, automotive coatings, and industrial paint [9], frequently in conjunction with inorganic white pigments as substrates.

In the literature, several works focus on the photoaging of synthetic organic pigments, in a powdered state [15] or when combined with binders [16], [17]. However, these studies mainly concentrate on molecules employed as textile dyes [18]. Raman spectroscopy has been extensively applied to the thorough examination and characterization of monoazo and isoindoline pigments, particularly in the context of their use in modern and contemporary paintings [19]-[21]. Despite the investigation of photoaging within the same molecular class [16], [22], a comprehensive study of the degradation processes specific to these pigments remains not fully understood.

This research is part of a larger investigation on the interaction between pigments and inorganic substrates - basic lead carbonate, titanium dioxide, and zinc oxide – aiming to study their stability and reactivity over time. The choice of these matchings is coherent with the historical employment of both white and yellow pigments. Despite the synthetic nature of the two selected yellow pigments, thus a late introduction on the trade, they were used in combination with lead white as well due to the permanence of the latter in the art materials trade after the laws prohibiting its application in paintings in the '60s [23]-[25]. Indeed, it has been possible to find artworks with lead white throughout the twentieth century [26], until it was almost completely replaced by the more common zinc and titanium white [27]. The investigation involved samples prepared both in layers and directly mixed. Specifically, the current work relates the aging process in bilayer systems in presence of the mentioned highly reactive metal components used as white substrates with the binder [28]-[30]. The investigation of such bilayer mock-ups, also involved the comparison with single paint samples, simply made up of yellow powders with the same binder. The aim lies in understanding the aging dynamics of materials in artifacts where both organic and inorganic elements coexist [31], [32]. To study the mechanisms of degradation, different analytical techniques are employed [33]. The investigation into physicochemical variations in bilayer samples involves a comprehensive approach, combining colorimetry, Fourier-transform infrared spectroscopy in attenuated total reflectance mode (ATR-FTIR), Raman spectroscopy (RS), and photoluminescence spectroscopy (PL). In particular, a special attention was given to correlating data obtained with PL spectroscopy and colorimetry, in order to clarify the link between spectroscopic information on molecular changes and macroscopic perceivable variations of the color [34].

2. MATERIALS AND METHODS

2.1. Materials

Monoazo Pigment Yellow 1 (referred also as Primary Yellow, C0001, PY 1), isoindoline Pigment Yellow 139 (referred also as Indian Yellow, C1998, PY 139), and linseed oil (Cold pressed Linseed oil, Art.3310/) were acquired from Zecchi (Zecchi - Colori Belle Arti, Florence, Italy). Lead carbonate (lead(II) carbonate basic -325 mesh), Titanium dioxide (titanium(IV) oxide, a mixture of rutile and anatase in nano powder form with < 100 nm particle size (BET), 99.5 % trace metal basis), and Zinc oxide (zinc oxide, puriss. p.a., ACS reagent, ≥ 99.0 % (KT)) were acquired from Sigma (Merk Life Science S.r.l. | Italy - Sigma-Aldrich). Lead white predominantly contains a composition of cerussite and hydrocerussite, titanium white is a blend of anatase and rutile, and zinc white mainly consists of the wurtzite phase. Figure 1 reports a representation of the pigments and their corresponding chemical structures.

2.2. Samples preparation

The samples preparation process is provided schematically on the right side of Figure 1. Reference samples containing only powder pigments were prepared using a procedure involving isopropyl alcohol [15], momentarily suspending the pigments and subsequently depositing them onto glass slides. The reference sample containing only linseed oil was prepared and air-dried for one month. Blending the powders of monoazo and isoindoline pigments with linseed oil, samples of single oil paint were realized, utilizing a powder-to-binder mass ratio of 1:2, and subsequently left to dry under room conditions for one month. Three bilayer paint samples were also realized for each yellow pigment in conjunction with the white pigments. A pair of oil

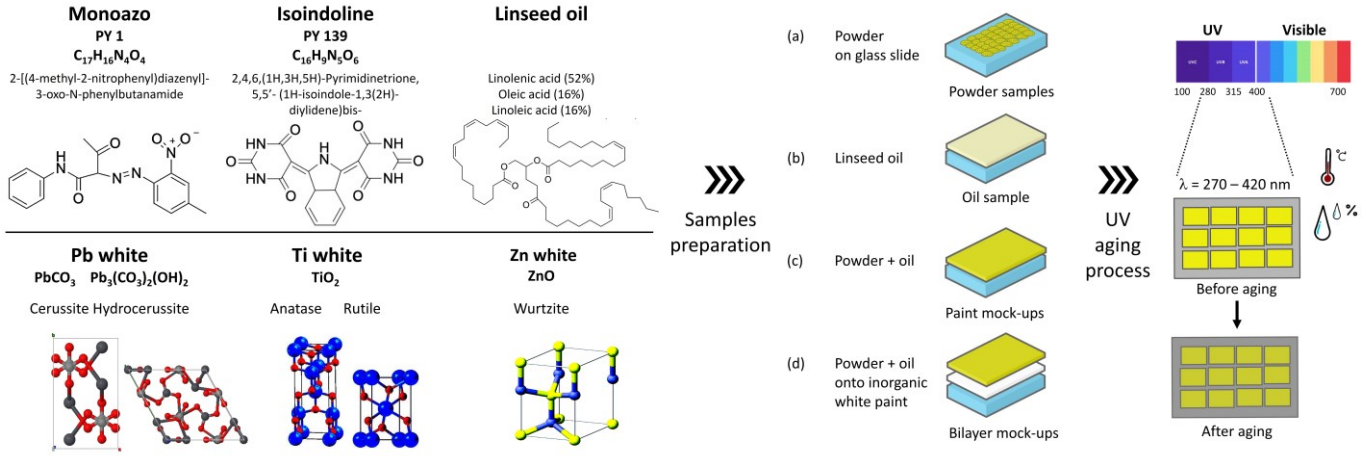

Figure 1. Materials (left) and the samples preparation with artificial aging process (right). The materials are presented at the top by the organic pigments of monoazo PY 1 and isoindoline PY 139 with their Colour Index names, molecular formulas, chemical names, and molecular structures. Additionally, linseed oil is featured with its predominant fatty acid components. At the bottom, the inorganic pigments, specifically lead carbonate basic, titanium dioxide, and zinc oxide, are accompanied by their molecular formulas and principal molecular structures. Sample preparation: (a) powder deposition on a glass slide, (b) linseed oil reference, (c) a single layer of oil paint (consisting of powder mixed with oil), (d) bilayer mock-ups created with a first layer of white inorganic pigment combined with oil for the each of the two yellow pigments. Finally, for the aging process UVB lamps emitting in the range 270-420 nm were employed, in controlled levels of temperature and relative humidity.

paint samples for each inorganic white pigment was prepared, allowing them to air-dry for one month under room conditions, and subsequently employing them as substrates for the application of one of the yellow pigments mixed with oil. In this way, bilayer mock-ups were made up of a layer-by-layer deposition of inorganic white pigment and organic yellow pigment using linseed oil as a binder. The resulting paint layers exhibited an approximate thickness ranging between 400-500 μm, using calipers (estimation over the sample set).

2.3. Artificial aging process

The artificial aging process, shown schematically in Figure 1 - right side, was conducted for 665 hours within a custom-designed aging chamber. Four UVB Broadband lamps (TL 20W/12 RS SLV/25, Philips Lighting) [35] were used, emitting maximal spectral power at 320 nm. The nominal value of the irradiance calculated by Keitz's formula [36] was 50.264 W/m^2. The temperature and the relative humidity were carefully maintained at approximately 30 °C and within the range of 70-90 %, respectively, via saturated solutions of NaCl in distilled water [37], [38]. A Grove – Temperature and Humidity Sensor DHT1 was placed on the surface of the aging box to monitor the parameters of temperature and relative humidity. Following aging, the samples were kept at room temperature for a week to stabilize them, before carrying out the experimental analyses.

2.4. Methods

Colorimetry was conducted by Eoptis CLM-194 instrument, a portable digital colorimeter. Colorimetric data were acquired in the CIE 1976 L*a*b* color space by the CLM-19X software with a standard D65 daylight illuminant and 10° observer. The geometry and the measurement area on the sample were fixed at 45° and 10 mm, respectively. The total color change ΔE was calculated as the root sum square of differences between the colorimetric parameters considered after and before aging [39], with the uncertainty calculated via the error propagation. An observer can notice a clear difference in color if $\Delta E > 3.5$ [40].

μ-ATR infrared spectroscopy was carried out with a ThermoFisher ®Nicolet iS50 FTIR Spectrometer with ®Nicolet Continuum Infrared Microscope. A 15 x objective on Microscope equipped with a germanium crystal tip and MCT/A detector was used. μ-ATR spectra, obtained as a sum of 120 scans in the range of 4000-650 cm^{-1} with a spectral resolution of 8 cm^{-1}, were collected and processed using Omnic 6.0 software.

Photoluminescence spectroscopy was carried on with Edinburgh Instruments FLS1000-SS with a Steady State Spectrometer. The spectrometer is equipped with Excitation and Emission monochromators, which allow the selection of a specific wavelength, the intensity of the light beam, and the bandwidth. A 450 W Xenon Arc Lamp as a light source and a visible PMT-980 as a detector were used to collect excitation and emission spectra, at room temperature and in front-face geometry configuration. Data acquisition and processing were conducted using Fluoracle 1.9.1 Software.

Raman measurements were obtained using a ®Renishaw Raman InVia Reflex Micro-Spectrometer, equipped with a CCD detector (10240 × 256 pixels, Peltier cooled cells at -70°C). Spectra were collected in backscattered configuration and with high pass Edge filter. Samples were investigated under a Leica DM 2700 M confocal microscope (20 ×, 50 × and 100 ×). A diode laser (785 nm) operates at an output power of 180 mW. The spectra were recorded at room temperature in the spectral range between 100-3800 cm^{-1}, with a nominal spectral resolution of about 1 cm^{-1}, by using a long working distance 50× objective, providing a laser spot size of about 2 μm^2. The laser power was varied depending on the sample analysed in the range of 0.5-100 % of the output power. Raman spectra were collected and elaborated with Wire 5.2 software.

3. RESULTS AND DISCUSSION

3.1. Powder samples

Figure 2 shows the colour changes following artificial aging, denoted by the ΔE values for the powder samples. Table 1 shows the results for the two yellow powder samples. In general, the a* components increased, whereas a reduction in the L* and b* parameters was detected. These numeric variations led to a loss of the red and yellow components, concomitant with a darkening of the overall colour. Notably, the most unstable pigment, showing post-aging colour change, was the yellow pigment PY 1 with a ΔE approaching 30. This effect is predominantly attributable to a significant decrease in the yellow component, as evidenced by the calculated Δb^*, with consequent perceptible darkening of the colour, as seen in Figure 2. As for the isoindoline PY 139, the total colour change ΔE was slightly exceeding 1, demonstrating remarkable light stability.

FTIR analyses in ATR mode for the pure powder samples are shown in Figure 3. By comparison of the spectra acquired before and after aging, the monoazo PY 1 powder sample showed a clear intensity increase in the higher wavenumbers' region, around 3500-3400 cm^{-1}, associated with O-H stretching. The presence of the same signals in the pre-aging spectrum, although less intense, could reasonably be due to surface water adsorption of the powder pigment, because of the polarity of PY 1. The rise of a new broadband at 1745 cm^{-1}, due to C=O groups, and a new intense band around 1150-1000 cm^{-1}, associated with C-O stretching, were also observed. This band underlies the peaks of

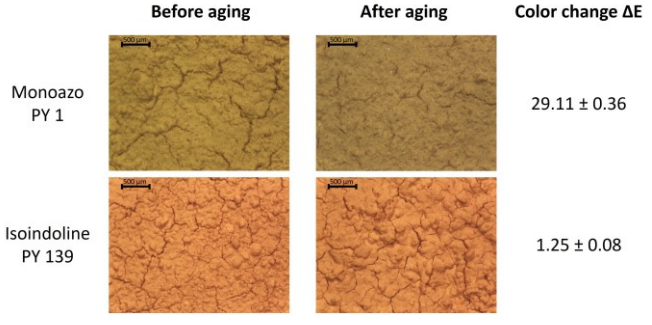

Figure 2. Images of the surfaces of powder samples before and after 665h aging with the total color changes ΔE calculated with colorimetry.

Table 1. Colorimetric shift Δ*L**, Δ*a**, Δ*b** after 665 h artificial aging for the yellow samples.

	Samples	Δ*L**	Δ*a**	Δ*b**
PY 1	Powder	-1.83 ± 0.02	4.80 ± 0.02	-28.57 ± 0.03
	Oil paint	-4.67 ± 0.15	4.03 ± 0.35	-8.34 ± 0.24
	Pb white	-5.78 ± 0.20	5.68 ± 0.18	-10.96 ± 0.14
	Ti white	-5.66 ± 0.06	5.09 ± 0.05	-11.82 ± 0.12
	Zn white	-5.40 ± 0.05	4.19 ± 0.12	-12.48 ± 0.16
PY 139	Powder	-0.07 ± 0.04	1.25 ± 0.04	-0.05 ± 0.06
	Oil paint	-2.44 ± 0.06	2.04 ± 0.07	-8.60 ± 0.37
	Pb white	-2.85 ± 0.14	2.47 ± 0.12	-16.65 ± 0.36
	Ti white	-2.45 ± 0.03	3.12 ± 0.08	-19.19 ± 0.26
	Zn white	-2.28 ± 0.04	2.37 ± 0.11	-22.02 ± 0.16

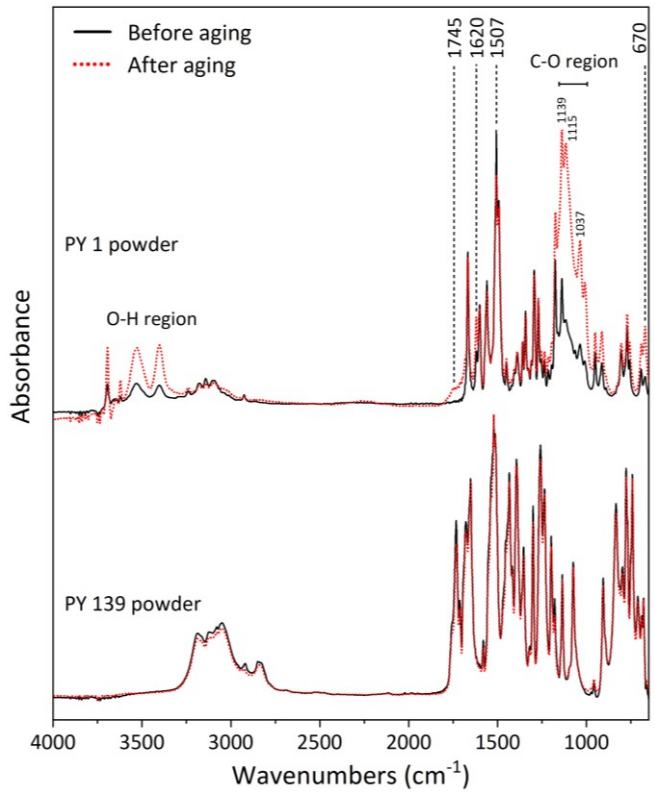

Figure 3. ATR-FTIR normalized spectra in the wavenumber range 4000-650 cm^{-1} for the powder samples: monoazo PY 1 and isoindoline PY 139 powder. Spectra acquired before aging are represented in black as a solid line, and those acquired after aging are in red as dots.

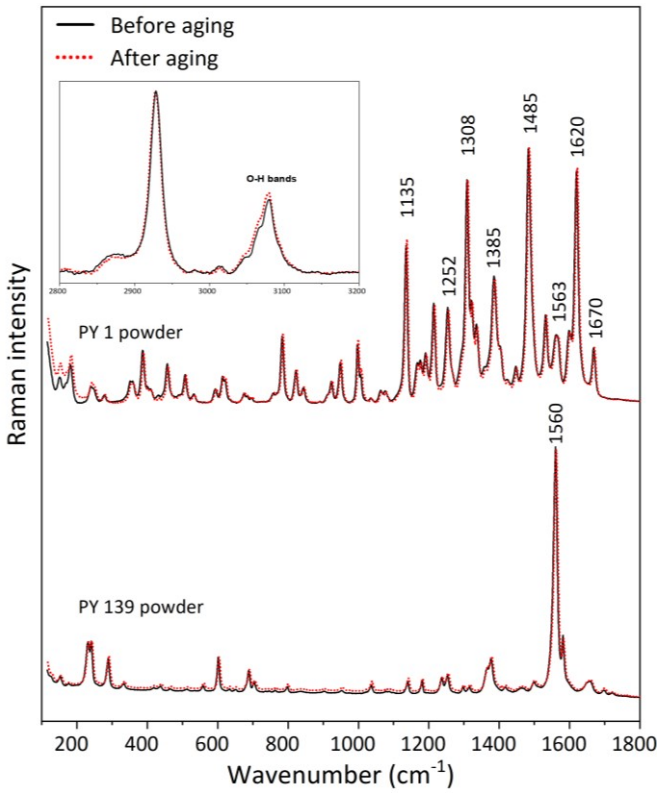

Figure 4. Normalized Raman spectra in the wavenumber range 100-1800 cm^{-1}, for the powder samples of monoazo PY 1 (with the inset in the range 2800-3200 cm^{-1}) and isoindoline PY 139. Before (black line) and after (red dots) aging spectra were acquired with the laser at 785 nm, setting the laser power at 7 mW for the PY 1 and 2.5 mW for the PY 139, with an integration time of 10 seconds, and 5 accumulations.

the monoazo pigment (as 1139 cm^{-1}, 1115 cm^{-1}, and 1037 cm^{-1} related to C-N and N=N stretching). Additionally, an increase of the signal at 1620 cm^{-1}, a reduction of the peak intensity at 1507 cm^{-1} and an increase of the signal at 670 cm^{-1}, were observed after aging. These variations were attributed to the O-H bending, the aromatic stretching of -C=C, and the out-of-plane O-H bending, respectively. The intensity variation observed in the O-H related signals could be due to the reaction of the pigment molecules with hydroxyl radicals. These radicals are probably formed by the interaction of UV radiation with water molecules present in the chamber as a consequence of the high relative humidity kept during the aging process. The added O-H groups are expected to cause a positive mesomeric effect M+ [41]. The newly formed stretching band of C-O in the fingerprint region is thus the consequence of such hydroxyls. These observations are consistent with the colorimetric analyses. Indeed, an increase in O-H signals would lead to a loss of the yellow component b*. As regards the isoindoline PY 139 powder sample, the spectra are perfectly superimposable in the fingerprint region (1800-650 cm^{-1}), underscoring that the isoindoline molecules have a robust lightfastness. Infrared analyses further suggest that the variations in O-H groups, causing colour changes in pigment PY 1, did not occur in pigment PY 139. This could be explained by a higher reactivity of the monoazo pigment due to the presence of the nitro -NO_2 group, causing polarity in the molecule, in opposition to the symmetry of the PY 139 molecule.

The monoazo PY 1 and the isoindoline PY 139 powders show the characteristic Raman spectrum in the spectral range 100-1800 cm^{-1}, Figure 4. For the monoazo PY 1 several strong bands are observed: the band at 1135 cm^{-1} is due to the C–N symmetric stretching, the band at 1252 cm^{-1} is due to the amide III bond mode, the band at 1308-1335 cm^{-1} is due to the aromatic nitro group, the band at 1385 cm^{-1} is due to the N=N stretching, the very strong band at 1485 cm^{-1} is due to the azobenzene ring, the band at 1563 cm^{-1} is due to amide II, the band at 1620 cm^{-1} is due to the nitro asymmetric stretch, the band at 1670 cm^{-1} is due to the amide I bond mode. Conversely to the IR spectrum, the variation due to the O-H vibrations in the Raman spectrum is negligible (inset in Figure 4) and C-O bonds were not detected. As regards the isoindoline PY 139, the Raman spectrum shows few characteristic signals with a strong band at 1560 cm^{-1} assigned to the amide II [20], [21]. By comparing Raman spectra, before and after aging, a perfect superposition of the characteristic bands is evident, setting the same experimental conditions measurement. This result shows that no damage is caused by artificial aging, confirming the photostability of the isoindoline pigment.

Photoluminescence activity was not observed for the monoazo pigment PY 1, probably due to the quenching process of the molecule which is common in the solid state [42]. Indeed, it was not possible to acquire an excitation spectrum and the corresponding emission spectrum at maximum excitation, as the pigment re-emitted only at the resonance peak ($\lambda_{ex}^{max} = \lambda_{em}^{max}$) [43]. On the contrary, a characteristic luminescence for the yellow isoindoline PY 139 is observed, in agreement with its strong fluorescence band in the yellow range [44]. Before and after aging emission scans of PY 139 powder are reported in Figure 5. The isoindoline PY 139 displayed a band with maximum emission at 572 nm with excitation wavelength at λ_{ex} = 530 nm, which only slightly changes following aging (solid and dashed orange lines).

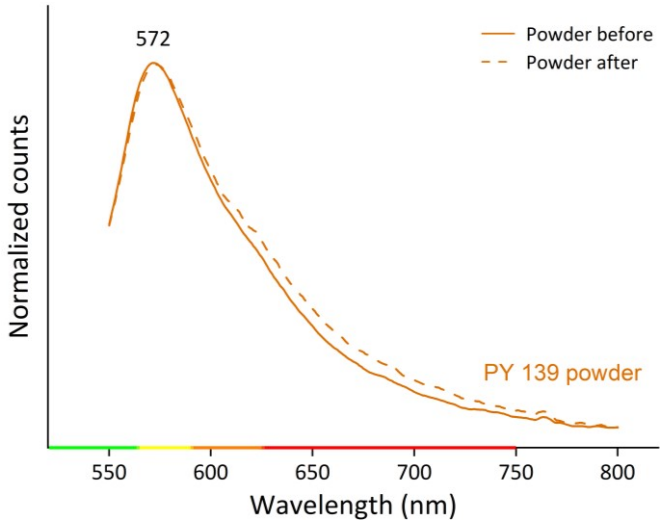

Figure 5. Emission scans in the range 550-800 nm for the isoindoline PY 139 powder sample at λ_{ex} = 530 nm. The scans were performed both before (solid line) and after (dashed line) aging process.

3.2. Paint mock-ups

In contrast to powders, PY 1 and PY 139 + oil samples proved a similar trend, as shown by the colour changes ΔE reported in Figure 6. Also in this case, for both samples, the main change is given by a loss of yellow component b^*, resulting in an overall darkening of the oil paint. By adding oil binder to the samples, the PY 1 + oil paint showed a lower loss of the yellow component b^* compared to the pure powder sample, while the isoindoline paint presented the opposite behaviour. Indeed, the PY 139 + oil samples showed a large loss of yellow component whereas its powder showed light stability.

The oil paint mock-ups were also studied with ATR-FTIR. As shown in Figure 7, the spectra obtained for the paint samples were compared with that of the single binder. After the aging, the ATR-FTIR spectrum of monoazo PY 1 + oil closely resembles that of the aged pure linseed oil. On the contrary, the spectrum of isoindoline PY 139 + oil preserved some spectral features of the pigment. As shown in Figure 7, before aging the FTIR spectral signals related to the yellow pigments were visible together with those of the oil. However, following aging, the predominant oil signals covered the contribution of the monoazo pigment, whose features were no longer evident. This common evidence could be due to a higher IR absorption of the aged oil compared to the monoazo PY 1, possibly as a consequence of increased density of the mixture resulting from the new extended cross-links net in the binder [45]. Furthermore, this effect could also be due to a greater contact of the ATR crystal tip with the binder, due to a lower availability of pigment powder on the aged surface of the sample compared to before aging, as shown in Figure 6. Conversely this effect is not found in the isoindoline PY 139 and the difference could rely in a higher IR absorbance of the pigment compared to the oil, as also observed in the pre-aging spectrum. All the variations observed in the spectra were consistent with an oxidative polymerization process inherent to the oil binder [46], [47]. These variations included an increase in the band at 3460 cm^{-1} associated with O-H stretching, a decrease at 2929-2856 cm^{-1} in the symmetric and asymmetric C-H stretching vibrations, broadening and increase at 1740-1734 cm^{-1} in the C=O carbonyl stretching, and an increase in C-O stretching at 1240-1170 cm^{-1} in the glyceride's linkages. In the context of these paint mock-ups, the photo-

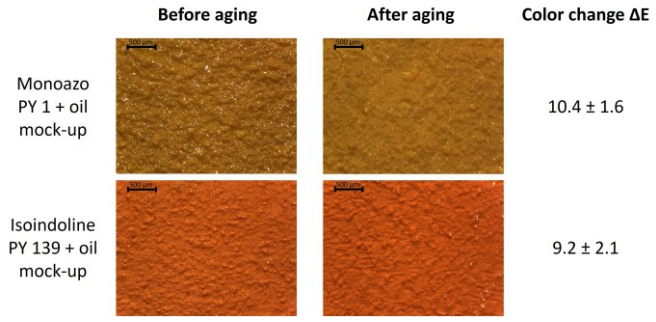

Figure 6. Images of the surfaces of oil paint mock-ups before and after 665h aging with the total colour changes ΔE calculated with colorimetry.

oxidation observed appears to be primarily attributable to the cross-linking of the oil binder [22], [48], being the O-H stretching increase compatible with the findings for PY 1 powder as well.

The comparison between the Raman spectra acquired before and after aging did not highlight a change in the characteristic bands of the pigments. The spectral contribution of the binder is not as appreciable as the pigment one due to the low intensity. Indeed, a perfect overlap of the spectra is visible, and no difference was recorded compared to the powder samples. This demonstrates that the accelerated aging did not likely give rise to any interaction between the pigment and the oil binder, as this would have resulted in visible modifications. The Raman spectrum of dried linseed oil sample is shown in Figure 8. Before the artificial aging some bands are observed: the band in the range 800-1100 cm^{-1} assigned to CH in (CH=CH) out-of-plane bending (wagging), two band at 1304 and 1440 cm^{-1} assigned to CH_2 in-plane bending (scissoring), some overlapped bands at about 1630-1660 cm^{-1} assigned to stretching of C=C isolated,

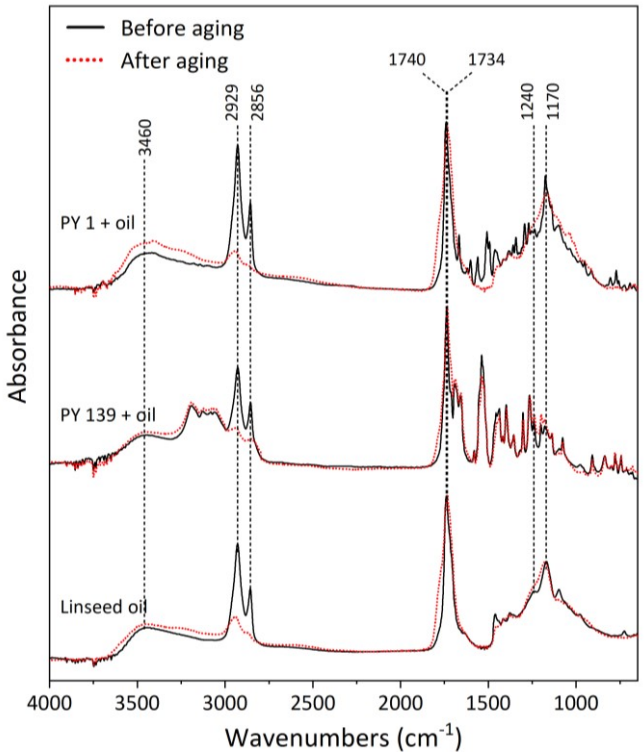

Figure 7. ATR-FTIR normalized spectra in the wavenumber range 4000-650 cm^{-1} for the oil paint samples: monoazo PY 1 + oil, isoindoline PY 139 + oil, and linseed oil reference. Spectra acquired before aging are represented in black as a solid line, and those acquired after aging are in red as dots.

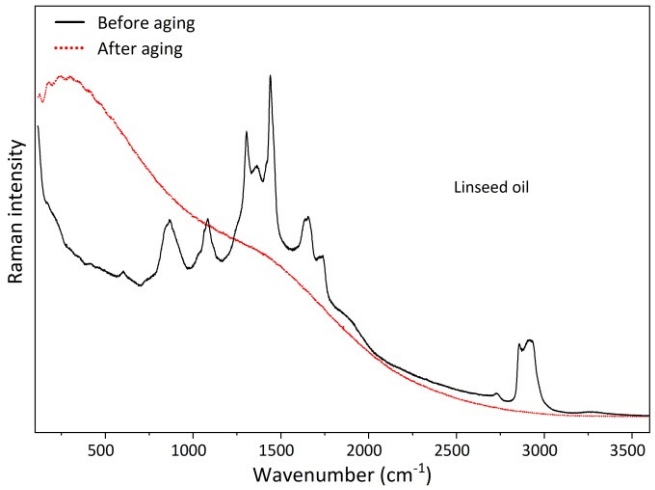

Figure 8. Normalized Raman spectra in the wavenumber range 100-3600 cm^{-1}, for the dried linseed oil sample, before (black line) and after (red dots) aging. Spectra were acquired with the laser at 785 nm, setting the laser power at 7 mW, with an integration time of 10 seconds, and 5 accumulations.

isolated cis and conjugated trans [49]. All these bands are typical for linoleic acid. Moreover, in the spectral range between 2690-3000 cm^{-1}, overlapping bands are present assigned to symmetric and asymmetric C–H stretching in methyl and methylene groups. After aging, fluorescence effect is predominant over any Raman diffusion. When oil is present in the paint mixture, the fluorescence in the aged samples does not affect the Raman spectrum, as it is dominated by the very intense signals of the yellow pigments.

Clear emission scans were obtained by photoluminescence after adding the oil to the samples for the paint mock-ups. Figure 9 shows the emission scans for the PY 1 oil paint sample acquired before and after aging, represented by the solid and dashed brown lines. A notable shift in the emission band was observed, wherein, at the same excitation wavelength λ_{ex} = 450 nm, the maximum emission exhibited a change from 537 nm to 545 nm, constituting a bathochromic shift of approximately 8 nm. The extent of the areas between the curves in Figure 9 on both sides is in accordance with what has been observed in colorimetry. The increase of intensity at higher wavelengths

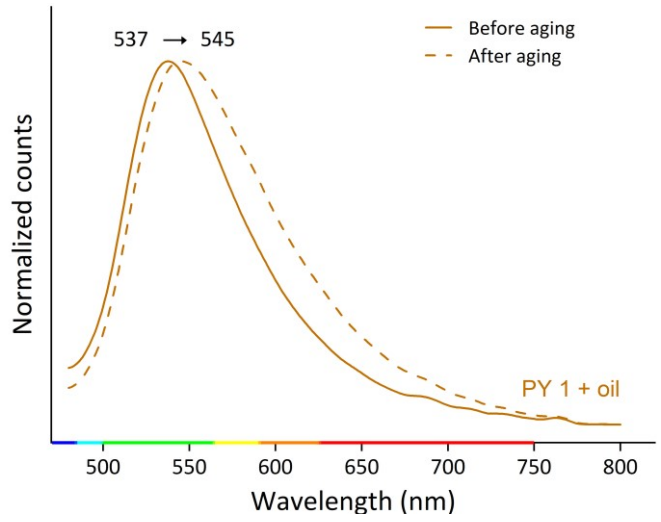

Figure 9. Emission scans in the range 480-800 nm acquired for the monoazo PY 1 + oil sample at λ_{ex} = 450 nm. The scans were performed both before (solid line) and after (dashed line) aging process.

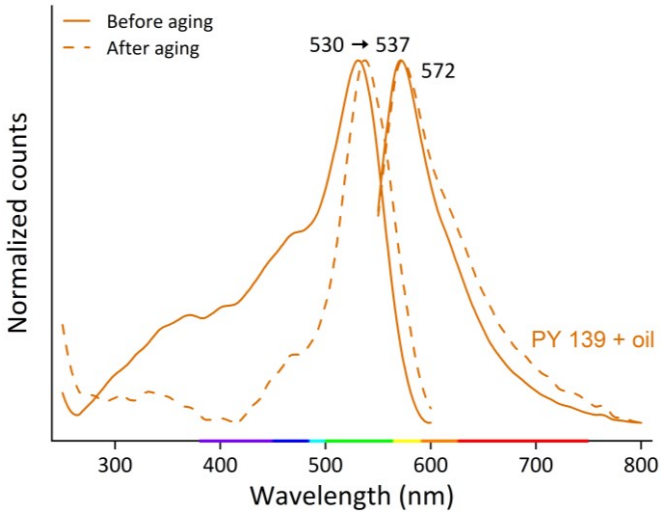

Figure 10. Excitation-emission scans for the isoindoline PY 139 + oil, in the excitation range of 250-600 nm and the emission range of 550-800 nm at λ_{ex} = 530 nm. The scans were performed both before (solid line) and after (dashed line) aging process.

entails the contribution to the red perception of the final colour. On the left side of the same curves, a decrease in the contribution of the green intensity is found. It should be stressed that this result cannot be discovered directly in the numeric colorimetric parameters L^*, a^*, b^* but must be attempted in the colour space diagram, as the colour domains are not equally distributed in the space [40]. Regarding the PY 139 paint sample, Figure 10 shows the comparison of excitation-emission scans before and after aging, represented by the solid and dashed orange lines. Similarly to the PY 1 paint sample emission scan, a broadening of the band towards longer wavelengths in the orange-red region can be found. In addition, upon aging, the excitation scan exhibited a bathochromic shift from 530 nm to 537 nm of the main band entailing higher yellow absorption. Finally, a strong decrease of the intensity below 525 nm was observed, leading to lower blue-green absorption and thus to higher reflection of these colours. Considering that both reflected and fluoresced lights contribute to the final perception of the colour [34], all these variations are in accordance with the hue of the aged sample which appears to be duller and more reddish as well. For both simple yellow paints, spectroscopic techniques indicate photooxidation predominantly affects the oil rather than the pigment. This keeps open the hypothesis of a protective action of the oil on the pigment.

3.3. Bilayer mock-ups

Figure 11 presents the total colour change for the bilayer samples. Following aging, the bilayer mock-ups with inorganic white substrates, exhibited colour changes with ΔE values ranging from 13 to 22. In the case of the bilayer samples with monoazo PY 1, the nature of the different metal oxides in the inorganic layer did not seem to significantly influence the colorimetric variations. Conversely, the effect on the PY 139 bilayer samples is significant. The most considerable variation in yellow-blue coordinate b* was observed for the samples prepared with zinc oxide compared to those prepared with titanium dioxide and lead carbonate. Due to the larger variation Δb^*, these samples appear darker on the surface of the paint layer.

The comparison between the ATR-FTIR spectra before and after aging respect to the corresponding single paint ones does not show significant discrepancies. Any saponification process due to the presence of inorganic metals was not detected [50],

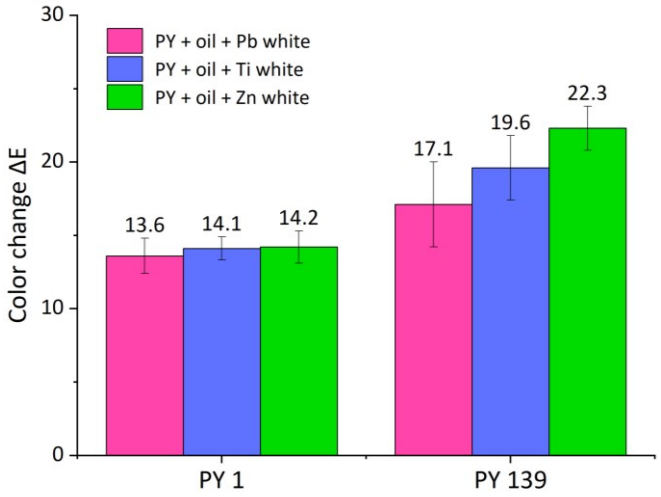

Figure 11. Color changes ΔE for the bilayer samples following artificial aging. On the left are the bilayer mock-ups realized with monoazo PY 1 and on the right are the bilayer mock-ups prepared with isoindoline PY 139.

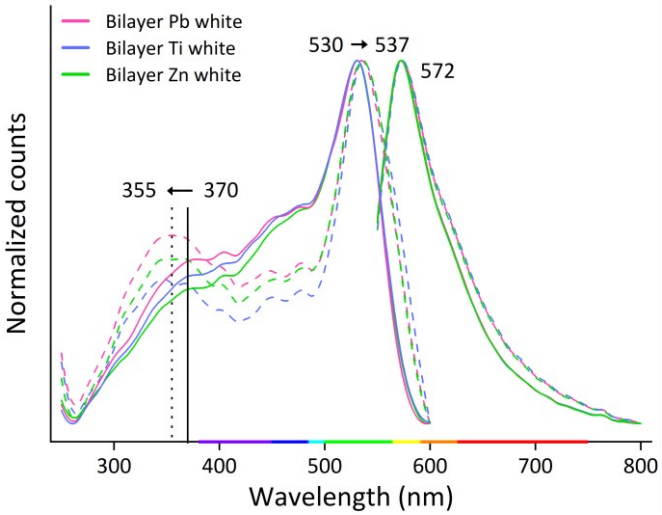

Figure 13. Excitation-emission scans for the bilayer samples with isoindoline PY 139, in the excitation range of 250-600 nm and the emission range of 550-800 nm at λ_{ex} = 530 nm. The scans were performed both before (solid line) and after (dashed line) aging process.

[51]. The aging time has probably not been enough to allow the saponification or the interdiffusion of the two compounds. Furthermore, the reaction could have occurred at the interface between the two layers, or the concentration of the metal soaps formed was too low compared to the predominant signals of the oil. In these cases, the analytical techniques are unable to investigate the formation of soaps.

From the analysis of the Raman spectra, performed before and after aging, no variations were observed between the bilayer samples and the samples with a single paint layer. This observation suggests that aging process did not induce any effect on the two yellow pigments, nor did it lead to interactions between the organic and inorganic layers of the paint.

After artificial aging, a shift of 10-15 nm towards longer wavelengths was observed in the emission spectra of the PY 1 bilayer samples, in Figure 12, similar to that observed in the simple paint PY 1 + oil. These spectral shifts suggest that samples in the presence of a layer with metal oxide underwent a more accelerated oil aging process. Indeed, these shift effects are wider than those previously observed in the single layer of oil paint sample with the monoazo pigment PY 1. Furthermore, the larger emission of the yellow-reddish components of the light is in accordance with the visible changes in the samples. In the case of isoindoline PY 139 bilayer mock-ups in Figure 13, all the emission bands centred at 572 nm exhibited the broadening towards longer wavelengths, due to aging. No significant deviations were observed among the different white pigments. Notable changes were observed in the corresponding excitation spectra, revealing a variability in intensity at 370 nm and a shift towards shorter wavelengths at 355 nm after aging. In the region of short wavelengths, the excitation signal at 370 nm is predominantly attributed to the aging of the oil [52]. Additionally, the main band at 530 nm presented a shift of about 7 nm. The observed red shift of the principal excitation band at 537 nm, together with an increase in intensity within the high-energy range at 370 nm and a decrease around 450 nm, denote a bathochromic, hyperchromic, and hypochromic effect, respectively [34]. These effects suggest that the UV radiation may induce faster aging in the oil binder when isoindoline PY 139 overlays an inorganic white substrate. Finally, the behaviour evidenced in Figure 13 is generally in good accordance with the more intense and dark orange colour of the aged samples: similarly to the previous comparisons, the area between each couple of unaged-aged curves means higher emission in the red region, higher absorption in the yellow range, and higher reflection in the blue-green region, being these contributions compatible with the colour variation above mentioned and the shift in the CIE 1976 L*a*b* colour space (not shown).

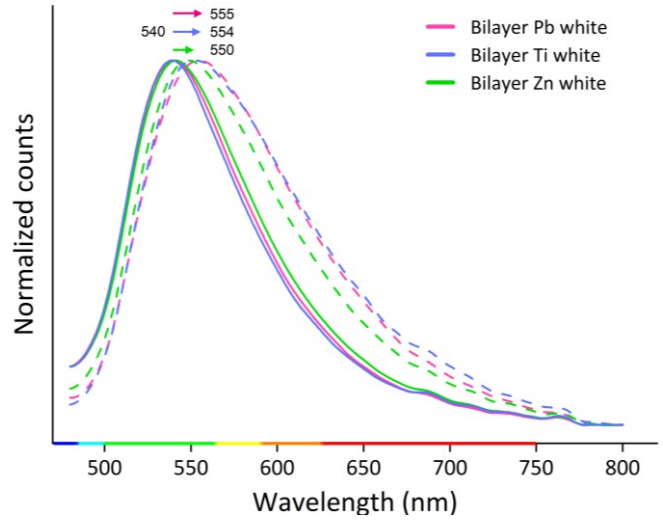

Figure 12. Emission scans for the bilayer samples with monoazo PY 1 in the excitation range of 480-800 nm at λ_{ex} = 450 nm. The scans were performed both before (solid line) and after (dashed line) aging process.

4. CONCLUSIONS

Among all the samples studied in this work, isoindoline powder PY 139 proved to be the only stable upon artificial aging, as the others showed minimum colour change ΔE = 9.2.

The aging carried out on the powder samples revealed an interaction between the monoazo powder PY 1 and OH• radicals, leading to a positive mesomeric effect M+ on the pigment molecules. All techniques used in this study confirmed the high stability of isoindoline powder PY 139 under the same aging conditions. From the analysis carried out, the two powder pigments react differently to the relative humidity activated by

UV radiation. This effect could be due to the different functional groups of the monoazo molecule PY 1, particularly the nitro group.

For the samples with the oil binder, there are no substantial colour changes ΔE between the two pigments. Indeed, no notable distinction was observed for the two yellow in the paint mock-ups. As shown by Raman spectroscopy, an interaction between the pigment powders (both monoazo and isoindoline) with the linseed oil binder was not recorded. However, Fourier-transform infrared spectroscopy revealed that all variations are consistent with the oxidative polymerization of the oil binder. This process was also detected in photoluminescence spectroscopy, where all the spectral changes observed are in agreement with the perceived colour after aging. If oil is added, it was hypothesized that the oil protects the pigment and therefore the pigments do not undergo variations due to aging. Both the yellow samples exhibited colour change $\Delta E > 8.0$ when mixed with oil, and can be ranked as fair or in class III lightfastness, worse than the ASTM classification.

The bilayer mock-ups exhibited greater sensitivity to changes in oil composition if compared to their simple paint sample. Specifically, the aging effect is more visible in the bilayer samples with isoindoline PY 139 than in those with monoazo PY 1, as denoted by the total colour change ΔE in Figure 11. Despite the multi-technique approach, it was not possible to understand the interaction between the organic-inorganic paint in the bilayer samples. Further investigations are therefore warranted for more information. Nevertheless, the results obtained with both photoluminescence spectroscopy and colorimetry lead to the conclusion that the inorganic layers may have caused a more accelerated drying of the oil binder, thus influencing the kinetics of the degradation processes.

REFERENCES

[1] A. van Loon, P. Noble, A. Burnstock, Ageing and deterioration of traditional oil and tempera paints, in: Conservation of Easel Painting. Routledge, London, 2020, ISBN: 978-0-7506-8199-5, pp. 214-241.

[2] C. Slottved Kimbriel, Colour change in paintings, Journal of the Institute of Conservation 40(3) (2017), pp. 267-269. DOI: 10.1080/19455224.2017.1360546

[3] R. L. Feller, Accelerated aging: Photochemical and thermal aspects, Getty Publications, 1995. ISBN 0-89236-125-5.

[4] C. Miliani, L. Monico, M. J. Melo, S. Fantacci, E. M. Angelin, A. Romani, K. Janssens, Photochemistry of artists' dyes and Pigments: Towards better understanding and prevention of colour change in works of art, Angewandte Chemie International Edition 57 (2018), pp. 7324-7334. DOI: 10.1002/anie.201802801

[5] E. Jablonski, T. Learner, J. Hayes, M. Golden, Conservation concerns for acrylic emulsion paints, Studies in Conservation 48 (2003) no. sup1: Reviews in Conservation 4, pp. 3-12. DOI: 10.1179/sic.2003.48.Supplement-1.3

[6] P.A. Lewis, Colorants: Organic and Inorganic Pigments, in: Color for science, art and technology. K. Nassau (editor). Elsevier, Amsterdam, 1997, ISBN: 978-0-4448-9846-3, pp. 283-312.

[7] S. L. Pugh, J. T. Guthrie, The development of light fastness testing and light fastness standards. Review of Progress in Coloration and Related Topics 31(1) (2001), pp. 42-56. DOI: 10.1111/j.1478-4408.2001.tb00137.x

[8] V. Pintus, S. Wei, M. Schreiner, UV ageing studies: evaluation of lightfastness declarations of commercial acrylic paints, Analytical and Bioanalytical Chemistry 402 (2012), pp. 1567-1584. DOI: 10.1007/s00216-011-5369-5

[9] S. Quillen Lomax, T. Learner, A Review of the Classes, Structures, and methods of analysis of synthetic organic pigments, Journal of the American Institute for Conservation 45(2) (2006), pp. 107-125. DOI: 10.1179/019713606806112540

[10] ASTM International, Standard Test Methods for Lightfastness of Colorants Used in Artists' Materials, Designation: D4303-03 (2003).

[11] David G. Myers. The color of art. Online [Accessed 22 August 2024] www.artiscreation.com

[12] J. van der Weerd, A. van Loon, J. J. Boon, FTIR Studies of the Effects of Pigments on the Aging of Oil, Studies in Conservation 50(1) (2005) pp. 3-22. Online [Accessed 20 September 2024] https://www.jstor.org/stable/25487713

[13] T. Poli, A. Piccirillo, M. Nervo, O. Chiantore, Ageing of natural resins in presence of pigments: metal soaps and oxalates formation, In: Metal Soaps in Art, Cultural Heritage Science, Springer, (2019), pp. 141-152. DOI: 10.1007/978-3-319-90617-1_8

[14] W. Herbst, K. Hunger, Industrial organic pigments, WILEY-VCH, Weinheim, 2004. ISBN: 3-527-30576-9.

[15] E. Ghelardi, I. Degano, M.P. Colombini, J. Mazurek, M. Schilling, H. Khanjian, T. Learner, A multi-analytical study on the photochemical degradation of synthetic organic pigments, Dyes and Pigments 123 (2015), pp. 396-403. DOI: 10.1016/j.dyepig.2015.07.029

[16] Z. E. Papliaka, K.S. Andrikopoulosb, E.A. Varella, Study of the stability of a series of synthetic colorants applied with styrene-acrylic copolymer, widely used in contemporary paintings, concerning the effects of accelerated ageing, Journal of Cultural Heritage 11(4) (2010), pp. 381-391. DOI: 10.1016/j.culher.2010.02.003

[17] M. Anghelone, V. Stoytschewb, D. Jembrih-Simbürger, M. Schreiner, Spectroscopic methods for the identification and photostability study of red synthetic organic pigments in alkyd and acrylic paints, Microchemical Journal 139 (2018) pp. 155-163. DOI: 10.1016/j.microc.2018.02.029

[18] M. P. Colombini, A. Andreotti, C. Baraldi, I. Degano, J. J. Łucejko, Colour fading in textiles: A model study on the decomposition of natural dyes, Microchemical Journal 85(1) (2007), pp. 174-182. DOI: 10.1016/j.microc.2006.04.002

[19] P. Ropret, S. S. Centeno, P. Bukovec, Raman identification of yellow synthetic organic pigments in modern and contemporary paintings: Reference spectra and case studies, Spectrochimica Acta Part A: Molecular and Biomolecular Spectroscopy 69(2) (2008), pp. 486-497. DOI: 10.1016/j.saa.2007.03.050

[20] A. Colombini, D. Kaifas, Characterization of some orange and yellow organic and fluorescent pigments by Raman spectroscopy, Proc. of the 8th international conference of the Infrared and Raman Users' Group (IRUG), Vienna, Austria, 26-29 March 2008, E-Preservation Science 7 (2010), pp. 14-21. Online [Accessed 22 August 2024] http://www.morana-rtd.com/e-preservationscience/2010/Colombini-02-04-2008.pdf

[21] W. Fremout, S. Saverwyns, Identification of synthetic organic pigments: the role of a comprehensive digital Raman spectral library, Journal of Raman Spectroscopy 43 (2012) pp. 1536-1544. DOI:10.1002/jrs.4054

[22] A. Ciccola, M. Guiso, F. Domenici, F. Sciubba, A. Bianco, Azo-pigments effect on UV degradation of contemporary art pictorial film: A FTIR-NMR combination study, Polymer Degradation and Stability 140 (2017), pp. 74-83. DOI: 10.1016/j.polymdegradstab.2017.04.004

[23] § 4.10.11 - Legge 19 luglio 1961, n. 706. Impiego della biacca nella pittura [in Italian]. Online [Accessed 27 August 2024]. https://www.edizioneuropee.it/LAW/HTML/26/zn4_10_011.html

[24] Council Directive 89/677/EEC, The Council of the European Communities, 21 December 1989. Online [Accessed 27 August 2024]. https://eur-lex.europa.eu/homepage.html
[25] U.S. Consumer Product Safety Commission, Lead-Containing Paint- Banned Hazardous Products, September 1977. Online [Accessed 27 August 2024]. https://www.govinfo.gov/
[26] R. Gettens, H. Kühn, W. Chase, Artists' Pigments—A Handbook of their History and Characteristics, vol. 2, Ashok Roy (editor), 1993, pp. 67-81, ISBN: 978-1-904982-75-3.
[27] T. J. S. Learner, P. Smithen, J. W. Krueger, M. R. Schilling, Modern Paints Uncovered: Proceedings from the Modern Paints Uncovered Symposium, Los Angeles: Getty Publications (editor), 2007, ISBN: 978-0-89236-906-5.
[28] I. Bonaduce, C. Duce, A. Lluveras-Tenorio, J. Lee, B. Ormsby, A. Burnstock, and K. J. van den Berg, Conservation Issues of Modern Oil Paintings: A Molecular Model on Paint Curing, Accounts of Chemical Research 52(12) (2019), pp. 3397-3406. DOI: 10.1021/acs.accounts.9b00296
[29] Z. Osawa, Role of metals and metal-deactivators in polymer degradation, Polymer Degradation and Stability 20 (1988), pp. 203–236. DOI: 10.1016/0141-3910(88)90070-5
[30] C. S. Tumosa, M. F. Mecklenburg, The influence of lead ions on the drying of oils, Studies in Conservation 50 (2005), pp. 39-47. DOI: 10.1179/sic.2005.50.Supplement-1.39
[31] M. Iorio, V. Graziani, S. Lins, S. Ridolfi, P. Branchini, A. Fabbri, G. Ingo, G. Di Carlo, (+ 1 more author), Exploring Manufacturing Process and Degradation Products of Gilt and Painted Leather, Applied Sciences 9(15) (2019), art. no. 3016. DOI: 10.3390/app9153016
[32] A. Sodo, L. Tortora, P. Biocca, A. Casanova Municchia, E. Fiorin, MA. Ricci, Raman and time of flight secondary ion mass spectrometry investigation answers specific conservation questions on Bosch painting Saint Wilgefortis Triptych, Journal of Raman Spectroscopy 50(2) (2019), pp. 150–160. DOI: 10.1002/jrs.5479
[33] L. Tortora, G. Di Carlo, M. J. Mosquera, G. M. Ingo, Editorial: Nanoscience and nanomaterials for the knowledge and conservation of Cultural Heritage, Nanoscience and Nanomaterials for the Knowledge and Conservation of Cultural Heritage, Frontiers in Materials 7 (2020), art. no. 606076. DOI: 10.3389/fmats.2020.606076
[34] K. Nassau, The physics and chemistry of color - The Fifteen Causes of Color, A Wiley-Interscience Publication, K. Nassau (editor), 1983, ISBN 0-471-86776-4.
[35] C. Cardell, A. Herrera, I. Guerra, N. Navas, L. Rodríguez Simón, K. Elert, Pigment-size effect on the physico-chemical behavior of azurite-tempera dosimeters upon natural and accelerated photo aging, Dyes and Pigments 141 (2017), pp. 53-65. DOI: 10.1016/j.dyepig.2017.02.001
[36] M. Sasges, J. Robinson, F. Daynouri, Ultraviolet lamp output measurement: A concise derivation of the Keitz equation, Ozone: Science & Engineering 34(4) (2012) pp. 306-309. DOI: 10.1080/01919512.2012.694322
[37] L. Greenspan, Humidity fixed points of binary saturated aqueous solutions, Journal of Research of the National Bureau of Standards - A. Physics and Chemistry 81A(1) (1977), pp. 89-96. DOI: 10.6028/jres.081A.011
[38] P. W. Winston, D. H. Bates, Saturated solutions for the control of humidity in biological research, Ecological Society of America 41(1) (1960) pp. 232-237. DOI: 10.2307/1931961
[39] R. T. Marcus, The measurement of color, in: Color for science, art and technology. K. Nassau (editor). Elsevier, Amsterdam, 1997, ISBN: 978-0-4448-9846-3, pp. 31-96.
[40] W. S. Mokrzycki, M. Tatol, Color difference Delta E - A survey, Machine Graphics and Vision 20(4) (2011), pp. 383-411. Online [Accessed 20 September 2024] https://wisotop.de/assets/2017/DeltaE-%20Survey-2.pdf
[41] G. Valitutti, Chimica Organica; Istituto Italiano Edizioni ATLAS, 1974. [in Italian]
[42] J. Plötner, A. Dreuw, Solid state fluorescence of pigment yellow 101 and derivatives: a conserved property of the individual molecules, Physical Chemistry Chemical Physics 8 (2006), pp. 1197-1204. DOI: 10.1039/b514815d
[43] D. A. Skoog, F. J. Holler, S. R. Crouch, Principles of instrumental analysis, Seventh edition, Sunder College Publisher, New York, 2017, ISBN: 978-1-305-57721-3.
[44] M. Longoni, A. Buttarelli, M. Gargano, S. Bruni, A multiwavelength approach for the study of contemporary painting materials by means of fluorescence imaging techniques: An Integration to Spectroscopic Methods, Applied Sciences 12(94) (2022). DOI: 10.3390/app12010094
[45] S. Pizzimenti, L. Bernazzani, M. R. Tinè, V. Treil, C. Duce, I. Bonaduce, Oxidation and cross-linking in the curing of air-drying artists' oil paints, ACS Applied Polymer Materials 3(4) (2021), pp. 1912-1922. DOI: 10.1021/acsapm.0c01441
[46] M. Lazzari, O. Chiantore, Drying and oxidative degradation of linseed oil, Polymer Degradation and Stability 65(2) (1999), pp. 303-313. DOI: 10.1016/S0141-3910(99)00020-8
[47] L. de Viguerie, P. A. Payard, E. Portero, Ph. Walter, M. Cotte, The drying of linseed oil investigated by Fourier transform infrared spectroscopy: Historical recipes and influence of lead compounds, Progress in Organic Coatings 93 (2016), pp. 46-60. DOI: 10.1016/j.porgcoat.2015.12.010
[48] V. Pintus, M. Schreiner, Characterization and identification of acrylic binding media: influence of UV light on the ageing process, Analytical and Bioanalytical Chemistry 399 (2011), pp. 2961-2976. DOI: 10.1007/s00216-010-4357-5
[49] A. Schönemann, H. G. M. Edwards, Raman and FTIR microspectroscopic study of the alteration of Chinese tung oil and related drying oils during ageing, Analytical and Bioanalytical Chemistry 400 (2011), pp. 1173–1180. DOI: 10.1007/s00216-011-4855-0
[50] M. Iorio, A. Sodo, V. Graziani, P. Branchini, A. Casanova Municchia, M. A. Ricci, (+ 3 more authors), Mapping at the nanometer scale the effects of sea-salt derived chlorine on cinnabar and lead white by using delayed image extraction in ToF-SIMS, Analyst 146(7) (2021), pp. 2392-2399. DOI: 10.1039/D0AN02350G
[51] P. Biocca, P. Santopadre, G. Sidoti, G. Sotgiu, F. de Notaristefani, L. Tortora, ToF-SIMS study of gilding technique in the fresco Vela della Castità by Giotto's school, ECASIA special issue paper: Surface and Interface Analysis 48(7) (2016), pp. 404-408. DOI: 10.1002/sia.5956
[52] L. K. Cairns, P. B. C. Forbes, Insights into the yellowing of drying oils using fluorescence spectroscopy, Heritage Science 8(59) (2020). DOI: 10.1186/s40494-020-00403-1